CFD for Micro-Scale Flows: Knudsen Slip Flow in a Micro-Channel

MSc Computational Fluid Dynamics
School of Aerospace, Transport & Manufacturing
Cranfield University
Author: Jamie Townsend, 239709
j.townsend@cranfield.ac.uk
Module Manager: Dr. László Könözsy
April 25, 2016
Word Count: 3014

Abstract

A two-dimensional micro-channel is used to simulate an ideal gas (air) at different Knudsen numbers (0.15 and 0.05) using a variety of modelling techniques near the wall to accommodate the transition away from the continuum hypothesis physics. The no-slip, Maxwell slip and a UDF (discretised Kandlikar slip model implemented in C) are simulated to study their effects. A mesh refinement was made to investigate its consequences, first and second order models were simulated for an analytical, Maxwell and UDF model. Varying constants were investigated for the second order models.

Nomenclature

Symbol	Meaning	SI Units
λ	Mean Free Path	m
μ	Dynamic Visocity	$kgm^{-1}s^{-1}$
ν	Kinematic Viscosity	m^2s^{-1}
ρ	Fluid Density	kgm^{-3}
σ	Momentum Accommodation Coefficient	-
ϕ	External Body Forces	$kgms^{-2}$
A_1	Constant	-
A_2	Constant	-
A	Cross-sectional Area	m^2
h	Channel Height	m
Kn	Knudsen Number	-
L	Characteristic Length	m
l	Channel Length	m
p	Pressure	Nm^{-2}
p_i	Inlet Pressure	Nm^{-2}
p_o	Outlet Pressure	Nm^{-2}
T	Temperature	K
t	Time	s
u_c	Cell Centre Velocity	ms^{-1}
u_s	Slip Velocity	ms^{-1}
u_w	Wall Velocity	ms^{-1}

1 Introduction

Computational Fluid Dynamics (CFD) is known to give scientists and engineers alike prescient information about a given fluid dynamics juncture in a variety of problem arrangements. The development of the field has extended beyond aerospace applications for example and can be readily applied to fluid dynamics problems involving the flow of bio-fluids in the human body, to the thermodynamics of flow within silicon-based technology. The latter two examples of CFD however can become problematic regarding the arrangement of the flow domain which consequently requires additional knowledge and modelling procedures that differ from external and many cases of internal flows. In particular, the concept of micro-flows can be introduced as a fundamental platform in which the investigation in this report encompasses.

A micro-channel, as classified by Mehendale *et al.* [1], details the range in which the flow occurs from 1 to $100\mu m$. Traditional theories imposed at this scale can differ the modelling process as a consequence of, [2, p.2]:

- Changes in the fundamental process, such as the continuum assumption becoming invalid and additional forces, such as electrokinetic forces becoming non-negligible.
- Uncertainty regarding empirical factors derived from experiments performed on large scales, such as entrance length.
- Uncertainty regarding measurements, such as geometrical dimensions and operating parameters.

Consider the initial point stated above, commonly the postulate that the material in a given control volume is a continuum and therefore continuously distributed throughout the domain of interest. The control volume must be smaller than the physical dimensions of the considered region, but it must be large enough to contain enough molecules to ensure any averaging of quantities such as velocity, pressure and density are meaningful, [3, p.3]. Intuitively one can comprehend that a lower limit to the size of a control volume exists for the continuum hypothesis to be valid.

As the flow moves away from the continuum state of flow, the flow, as well as being compressible, starts to creep and therefore appropriate models are needed for simulations to employ a slip condition rather than a no-slip condition as is commonly seen in many applications.

The continuum hypothesis also requires that thermodynamic equilibrium exists, that is, material properties are constant from point to point and there is no tendency for change in time, [3, p.5]. The mean free path is the average distance a molecule travels before it collides with another, [3, p.3]. To respect the thermodynamic equilibrium clause, the intermolecular collisions within the aforementioned control volume must be sufficiently high enough in frequency. It then stands to reason that the mean free path is small when compared to the characteristic length of the control volume. Therefore, thermodynamic equilibrium enforces the condition:

$$\frac{\lambda}{L} \ll 1 \tag{1.1}$$

Where λ is the mean free path and L is the characteristic length of the control volume. The Knudsen number can now be formally introduced as a means to determine whether the continuum hypothesis is valid for a given flow situation. The Knudsen number, denoted Kn, is a dimensionless number defined as, [2, p.16]:

$$\mathrm{Kn} = \frac{\lambda}{L} \tag{1.2}$$

A classification of flow regimes concerning their Knudsen number is made by Kandlikar *et al.* which should be noted is subtly manipulated by empiricism and is presented as, [2, p.18]:

- $\mathrm{Kn} < 10^{-3}$ indicates **continuum flow**, the compressible Navier-Stokes equations along with the classical no-slip boundary condition apply.
- $10^{-3} < \mathrm{Kn} < 10^{-1}$ indicates **slip flow**, the Navier-Stokes equations remain valid however a velocity slip and temperature jump must be accounted for at the walls.
- $10^{-1} < \mathrm{Kn} < 10$ indicates **transition flow**, the continuum approach of the Navier-Stokes equations are not valid.
- $\mathrm{Kn} > 10$ indicates **free molecular flow**, the intermolecular collisions are negligible compared to the collisions between gas molecules and the walls.

In the upcoming investigation presented in this report, pressure-driven slip flow in a micro-channel is studied to evaluate the magnitude of non-continuum effects. An analytical solution exists which shall be presented momentarily and can thus be used to determine the accuracy of the CFD findings. The baseline case problem parameters can be summarised as follows:

- Geometry: $(2h \times l) = (0.226 \times 5)\mu m$
- $P_i = 3\ atm$
- $P_o = 2\ atm$
- $T = 300K$, uniform
- Wall material: Aluminium
- Fluid: air, constant viscosity
- Baseline grid: $(2h \times l) \rightarrow 40 \times 100$

A problem schematic can be seen in figure 1.

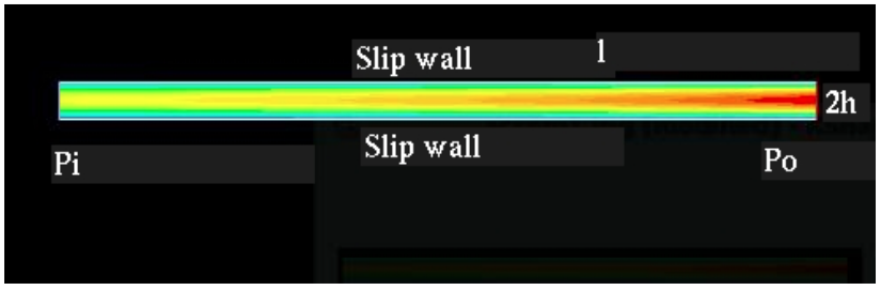

Figure 1: Problem Schematic

An ideal gas flow through the micro-channel is simulated using the no-slip condition, FLUENT's Maxwell slip condition and a User Defined Function (UDF) that enforces the slip condition by

Kandlikar, [2]. In addition to this, two Knudsen numbers are simulated to examine their effects, 0.05 and 0.15. It is thought via the previously mentioned theory that the latter Knudsen number will demonstrate slip/creeping flow with more emphasis.

2 Governing Equations & Analytical Solution

The governing equations are now presented with a derivation for the analytical solution implemented within this investigation, alongside two slip models, one pre-existing FLUENT model and a UDF model. In practice, the compressible Navier-Stokes equations are used within the simulation environment, however to derive the analytical solution, an incompressibility assumption is made. The compressible Navier-Stokes equations are presented as [4, p.41]:

$$\frac{\partial \boldsymbol{u}}{\partial t} + (\boldsymbol{u} \cdot \boldsymbol{\nabla})\boldsymbol{u} = -\frac{1}{\rho}\nabla p + \mu\nabla^2\boldsymbol{u} + \frac{1}{3}\nu\nabla(\nabla \cdot \boldsymbol{u}) + \boldsymbol{\phi} \tag{2.1}$$

The three-dimensional incompressible Navier-Stokes equations for the derivation of an analytical solution can be written as follows [4, p.32]:

$$\frac{\partial \boldsymbol{u}}{\partial t} + (\boldsymbol{u} \cdot \boldsymbol{\nabla})\boldsymbol{u} = -\frac{1}{\rho}\nabla p + \mu\nabla^2\boldsymbol{u} + \boldsymbol{\phi} \tag{2.2}$$

With a corresponding continuity equation:

$$div(\boldsymbol{u}) = \frac{\partial u}{\partial x} + \frac{\partial v}{\partial y} + \frac{\partial w}{\partial z} = 0 \tag{2.3}$$

Where $\boldsymbol{u} = (u, v, w)$ is the velocity in the x, y and z direction, respectively. p is the pressure, ρ is the fluid density, μ is the kinematic viscosity, t is the time, $\boldsymbol{\phi}$ is any external body forces and $\boldsymbol{\nabla}$ is the vector differential operator defined as:

$$\boldsymbol{\nabla} = \frac{\partial}{\partial x}\boldsymbol{e_x} + \frac{\partial}{\partial y}\boldsymbol{e_y} + \frac{\partial}{\partial z}\boldsymbol{e_z} \tag{2.4}$$

The investigation concerns the two-dimensional flow through the micro-channel, hence the Navier-Stokes can be reduced to:

$$\frac{\partial u}{\partial t} + u\frac{\partial u}{\partial x} + v\frac{\partial u}{\partial y} = -\frac{1}{\rho}\frac{\partial p}{\partial x} + \nu\left(\frac{\partial^2 u}{\partial x^2} + \frac{\partial^2 u}{\partial y^2}\right) + \phi_x \tag{2.5}$$

$$\frac{\partial v}{\partial t} + u\frac{\partial v}{\partial x} + v\frac{\partial v}{\partial y} = -\frac{1}{\rho}\frac{\partial p}{\partial y} + \nu\left(\frac{\partial^2 v}{\partial x^2} + \frac{\partial^2 v}{\partial y^2}\right) + \phi_y \tag{2.6}$$

Where ν is the dynamic viscosity ($\nu = \frac{\mu}{\rho}$) and with a corresponding two-dimensional continuity equation:

$$\frac{\partial u}{\partial x} + \frac{\partial v}{\partial y} = 0 \tag{2.7}$$

To further simplify equations (2.5) and (2.6) such than an analytical solution can be easily evaluated, the following assumptions about the fluid flow are made:

1. The fluid flow is steady/laminar $\Rightarrow \frac{\partial}{\partial t} = 0$

2. The fluid flow is uni-directional in the x-direction $\Rightarrow \boldsymbol{u} = (u, 0)$
3. The fluid flow is fully developed $\Rightarrow \frac{\partial u}{\partial x} = 0$
4. External body forces are negligible $\Rightarrow \phi_x = \phi_y = 0$

These assumptions then yield the following simplification (cancelled term numbers *below* correspond to numbers in the *above* list):

$$\underbrace{\cancel{\frac{\partial u}{\partial t}}}_{1} + \underbrace{\cancel{u\frac{\partial u}{\partial x}}}_{3} + \underbrace{\cancel{v\frac{\partial u}{\partial y}}}_{2} = -\frac{1}{\rho}\frac{\partial p}{\partial x} + \nu\left(\underbrace{\cancel{\frac{\partial^2 u}{\partial x^2}}}_{3} + \frac{\partial^2 u}{\partial y^2}\right) + \underbrace{\cancel{\phi_x}}_{4} \tag{2.8}$$

$$\underbrace{\cancel{\frac{\partial v}{\partial t}}}_{1} + \underbrace{\cancel{u\frac{\partial v}{\partial x}}}_{2} + \underbrace{\cancel{v\frac{\partial v}{\partial y}}}_{2} = -\frac{1}{\rho}\frac{\partial p}{\partial y} + \nu\left(\underbrace{\cancel{\frac{\partial^2 v}{\partial x^2}}}_{2} + \underbrace{\cancel{\frac{\partial^2 v}{\partial y^2}}}_{2}\right) + \underbrace{\cancel{\phi_y}}_{4} \tag{2.9}$$

Removing the cancelled terms yields:

$$0 = -\frac{1}{\rho}\frac{\partial p}{\partial x} + \nu\frac{\partial^2 u}{\partial y^2} \tag{2.10}$$

$$0 = -\frac{1}{\rho}\frac{\partial p}{\partial y}; \quad \frac{1}{\rho} \neq 0 \tag{2.11}$$

Equation (2.11) can then be solved for p, this consequently reveals that the flow pressure only acts in the x-direction.

$$\frac{\partial p}{\partial y} = 0 \Rightarrow p = p(x) + const. \tag{2.12}$$

Equation (2.10) can then be re-expressed to form the basis of the analytical solution:

$$\frac{d^2 u}{dy^2} = \frac{1}{\mu}\frac{dp}{dx} \tag{2.13}$$

The flow speed, $u(y)$, between the parallel plates at the positions $y = \pm h$ and $y = 0$ is given as:

$$u(y = \pm h) = -\frac{2 - \sigma}{\sigma}\lambda\frac{du}{dy} \tag{2.14}$$

$$\frac{du}{dy}(y = 0) = 0 \tag{2.15}$$

To obtain a general solution for $u(y)$, integration of equation (2.13) and re-writing the pressure derivative as the change in pressure Δp over the plate length L, this yields:

$$\begin{aligned} u(y) &= \frac{1}{\mu}\frac{\Delta p}{L}\iint dy^2 \\ u(y) &= \frac{1}{\mu}\frac{\Delta p}{L}\left[\frac{y^2}{2} + ay + b\right] \end{aligned} \tag{2.16}$$

Where a and b are constants to be determined via applying the appropriate boundary conditions. By substitution of the boundary condition from equation (2.15) into the general expression from equation (2.16), one finds that the value of the constant a is zero, $a = 0$. This yields:

$$u(y) = \frac{1}{\mu}\frac{\Delta p}{L}\left(\frac{y^2}{2} + b\right) \tag{2.17}$$

Next, one should consider the slip velocity which enables the determination of the velocity at the wall for first and second orders of accuracy, this can be written as, [2, p.28]:

$$u_s = A_1\lambda\frac{\partial u}{\partial y}\bigg|_h + A_2\lambda^2\frac{\partial^2 u}{\partial y^2}\bigg|_h \tag{2.18}$$

By then substituting the velocity profile in equation (2.17) into the slip velocity expression in equation (2.18), the following can be realised:

$$\begin{aligned} \frac{1}{\mu}\frac{\Delta p}{L}\left(\frac{y^2}{2} + b\right) &= A_1\lambda\left(\frac{b}{\mu}\frac{\Delta p}{L}\right) + A_2\lambda^2\left(\frac{1}{\mu}\frac{\Delta p}{L}\right) \\ \Rightarrow b &= \frac{1}{\mu}\frac{\Delta p}{L}\left(A_1 h\lambda + A_2\lambda^2 - \frac{h^2}{2}\right) \end{aligned} \tag{2.19}$$

This then gives rise to a final general expression for the velocity within the plates including a slip velocity at the wall regions:

$$\boxed{u(y) = \frac{1}{\mu}\frac{\Delta p}{L}\left(\frac{y^2}{2} + A_1\lambda h + A_2\lambda^2 - \frac{h^2}{2}\right)} \tag{2.20}$$

Where A_1 and A_2 are constants which are altered to decide what order of accuracy the analytical solution is to represent. For a first order result, the constant A_2 must be set equal to zero, when a second order result is required however, various values can be used, and are in fact studied within this investigation. The value of A_1 remains the same throughout which is $A_1 = 1$ and is derived through the first boundary condition shown previously in equation (2.14). A full table of the constants are discussed in table 1 in section 3.1.2.

ANSYS FLUENT has the built-in capability to use the **Maxwell slip condition**, the gas-surface interaction is represented by incidence and reflection where their combination yields an expression for the velocity slip in vector form, [5, pp.214-215].

Other such models exist, although not discussed in this report. Models such as the **Cercignani-Lampis** model was designed to give a more accurate description of the gas-surface interaction. The fundamental scattering kernel principles are said to be satisfied and the momentum and energy accommodations coefficients differ. The **Langmuir** model uses the effect of long range body forces derived from surface chemistry theory however is can be less physical regarding its performance, [6].

3 Methodology

The following methodology describes the acquisition of the UDF used in this investigation as well as a description for its use concerning a first and second order accurate model. Similarly, the same description is presented for the previously derived analytical solution. The method of altering the Knudsen number, Kn, is discussed, an explaination of the mass flow rate and how one would go about calculating such a quantity is described and finally the solver parameters used in ANSYS FLUENT are presented.

3.1 User Defined Function (UDF)

The UDF implemented in this investigation follows that of Kandlikar [2] and can be achieved for both first and second orders of accuracy using the following methodology. The velocity at the wall (u_w) can be expressed using slip velocity used *a priori* and is written as:

$$u_w = A_1\lambda\frac{\partial u}{\partial y} + A_2\lambda^2\frac{\partial^2 u}{\partial y^2} \tag{3.1}$$

Where A_1 and A_2 remain as arbitrary constants. The first and second order derivatives are then discretised using a forward and central differencing scheme, respectively. The schemes use values from the cell centres and values from the cell walls to achieve functionality, for the second order scheme, a *ghost* cell must be used to fully resolve the wall values of velocity. This can be expressed as follows:

$$u_w = 2A_1\lambda\frac{u_c - u_w}{\Delta y} + A_2\lambda^2\frac{u_c - 2u_w + u_w}{\Delta y^2} \tag{3.2}$$

Where u_c corresponds to the velocity at the centre of the current cell. A complete expression for u_w can then be obtained from equation (3.2) via careful algebra:

$$\boxed{u_w = \frac{u_c\lambda(2A_1\Delta y + A_2\lambda)}{(\Delta y^2 + 2A_1\lambda\Delta y + A_2\lambda^2}} \tag{3.3}$$

3.1.1 First Order Model

For a first order approximation, the constant value of A_2 seen in equation (3.3) must be set equal to zero. This gives rise to the following expression for the wall velocity, u_w:

$$u_w = \frac{2A_1u_c\lambda\Delta y}{\Delta y^2 + 2A_1\lambda\Delta y} \tag{3.4}$$

The value of the constant A_1 is then set equal to the boundary condition presented previously in section 2 from equation (2.14). In this case of a first order model, the value of σ can be assumed equal to 1, as has been done in various investigations, summarised by Barber *et al.* [7] and presented in table 1. One then finds an expression for u_w as:

$$\boxed{u_w = \frac{2u_c\lambda\Delta y}{\Delta y^2 + 2\lambda\Delta y}} \tag{3.5}$$

3.1.2 Second Order Model

For a second order approximation, the expression for u_w (equation (3.4)) in section 3.1.1 is used and implemented within the UDF code with varying values for the constant A_2, this is summarised in table 1 as follows with the value of A_1 remaining consistent with that of the first order model.

Author	**Date**	A_1	A_2
Maxwell [8]	1879	1	0
Schamberg [9]	1947	1	$5\pi/12$
Cercignani & Daneri [10]	1963	1.1466	0.9756
Deissler [11]	1964	1	9/8
Hsia & Domoto [12]	1983	1	0.5
Karniadakis & Beskok [13]	2002	1	-0.5
Lockerby *et al.* [14]	2004	1	0.15 - 0.19

Table 1: First and second order slip coefficients - literature survey from Barber *et al.*, [7].

First and second order UDF's can be seen in Appendix A and B, respectively.

3.2 Knudsen Number Modifications

In order to modify the Knudsen number of the flow, the value of the mean free path can also be expressed as, [2, p.26]:

$$\lambda = \sqrt{\frac{\pi}{2}} \frac{\mu}{\rho_o \sqrt{RT}} \tag{3.6}$$

Using the ideal gas law, ρ_o can be expressed as:

$$\rho_o = \frac{p_o}{RT} \tag{3.7}$$

Where the subscript o refers to the value at the outlet of the channel. By altering the pressure at the outlet in ANSYS FLUENT, the Knudsen number can be changed accordingly. Table 2 presents the values of pressure at the inlet and outlet with their corresponding Knudsen number required for this investigation.

Kn	p_i (atm)	p_o (atm)
0.15	3	2
0.05	6.74	5.74

Table 2: Knudsen numbers with their corresponding pressures needed at the inlet and outlet of the micro-channel.

3.3 Mass Flow Rate

As a means to analyse the flow, the mass flow rate is calculated. For the sake of completeness, the expression to calculate such a value is now presented. The mass flow rate is defined as, [15, p.72]:

$$\dot{m} = \frac{dm}{dt} = \rho A u \tag{3.8}$$

Where A is the cross-sectional area and u is the average velocity at a section of the flow.

3.4 Solver Parameters

In ANSYS FLUENT, a double precision, pressure-based solver was used. The flow was modelled as laminar and the energy equation was turned on. The boundary conditions imposed at the inlet and outlet were pressure-inlet and pressure-outlet, respectively, with pressure values corresponding to table 2 to implement the correct Knudsen number. The fluid was set to air as an ideal gas, the thermal accommodation coefficient and momentum accommodation coefficient were both set to 1.

To implement the no-slip condition, standard laminar flow was chosen and a stationary no-slip condition was applied.

To implement the Maxwell slip condition, laminar low-pressure boundary slip was applied.

To implement the UDF, it was loaded into ANSYS FLUENT, moving wall was chosen along with components and then the x-velocity could be chosen as a wall function.

The pressure velocity coupling was chosen to use the SIMPLE scheme, the spatial discretisation was selected as follows:

- Gradient: Least Squares Cell Based
- Pressure: Standard
- Density: First Order Upwind
- Momentum: First Order Upwind
- Energy: First Order Upwind

A solver parameter study showed that the above choices had little effect on the final results so the least computationally expense choices were made.

Additionally, the mesh was refined for one small investigation using ANSYS ICEM whereby the subsequent mesh is twice as fine such that the mesh has a size 80×200 cells.

4 Results & Analysis

The simulation results are now presented in turn, initially the four methods of modelling the flow in the near-wall region are presented: the analytical solution, the no-slip condition, the Maxwell slip condition and the implemented UDF. Additionally the simulations are performed using the two Knudsen numbers under investigation: Kn = 0.15 and Kn = 0.05. The respective results can be seen in figures 2 to 6. The mass flow rate has been calculated for each successive model and is presented alongside its deviation from the no-slip boundary condition values, seen in tables 3 to 5. For the second order velocity profiles, the coefficient A_2 is set to $5\pi/12$ as this was found to give the better results regarding overall accuracy, a summary of the deviations from the no-slip condition is presented in table 5 with varying values of A_2.

For the Knudsen number, Kn=0.05, the flow is beginning to move away from the typical continuum hypothesis an the flow can be seen to start to creep at the wall, this is presented in figure 2. Besides the no-slip model, the remaining models tend to agree with one another quite well, with the UDF providing the closest prediction to the analytical solution.

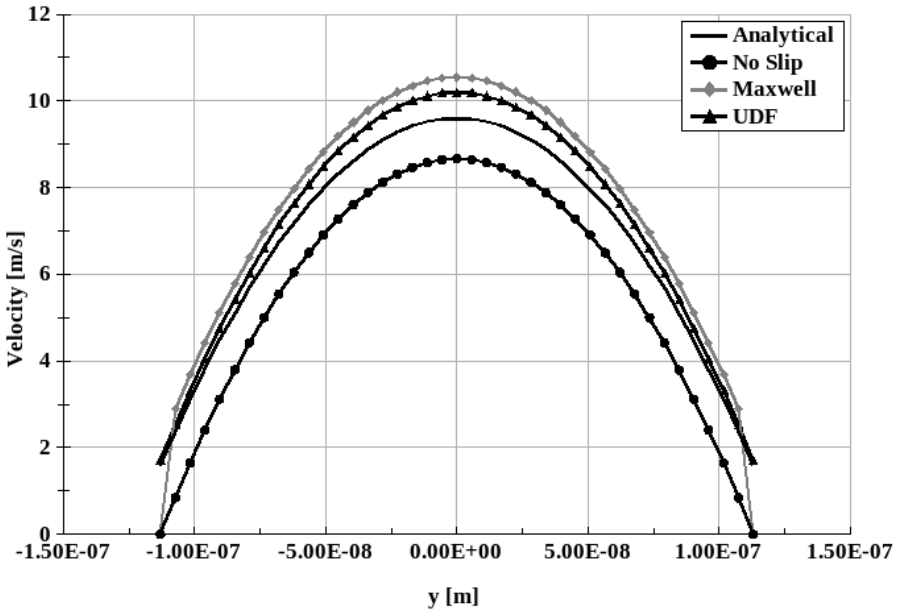

Figure 2: Kn = 0.05 first order analytical, Maxwell, no-slip and UDF velocity profiles.

For the Knudsen number, Kn = 0.15, it can be seen that the velocity profiles differ by approximately $2ms^{-1}$ between the no-slip and analytical model and approximately $1ms^{-1}$ between the analytical and Maxwell/UDF solution in figure 3. Although the UDF and Maxwell models over-predict the velocity in the channel, they do agree with one another which one would intuitively expect as the model equations are similar for a first order case. The no-slip model falls drastically short in prediction, this can be expected as a stationary flow is simulated at the wall, which would therefore hinder the velocity profile development. This flow is a transition flow, that is, it is farther from the continuum hypothesis approach than its smaller Knudsen number counterpart, and therefore the velocity at the near-wall region is higher.

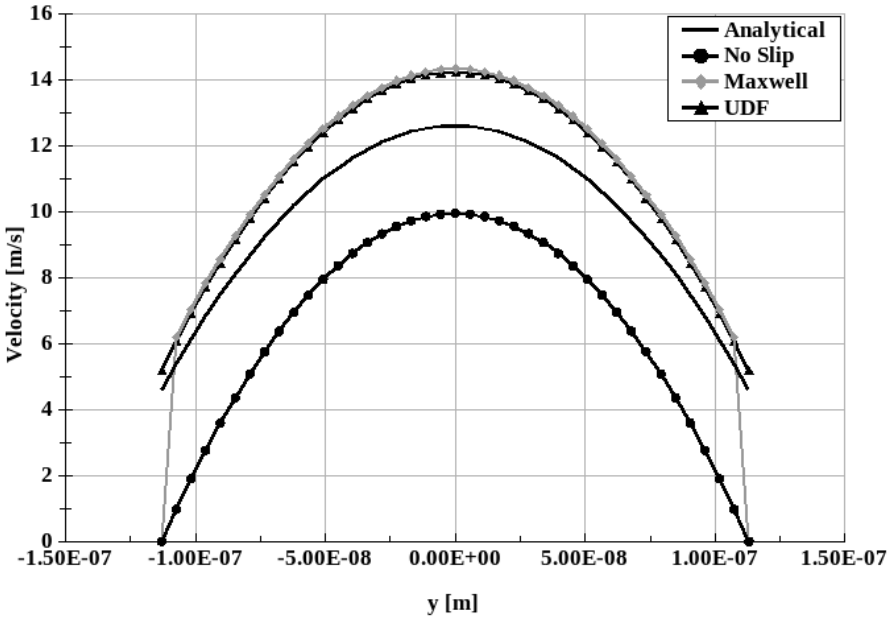

Figure 3: Kn = 0.15 first order analytical, Maxwell, no-slip and UDF velocity profiles.

The refined mesh was simulated using a Knudsen number of Kn = 0.15 investigated using the same aforementioned models and can be seen in figure 4. It was found that the results became vastly different from one another, the UDF being the worst offender and over-predicting the velocity profile by approximately 4 ms^{-1} at the peak. The Maxwell model fell short from the analytical solution and the no-slip continued this trend of under-prediction more so.

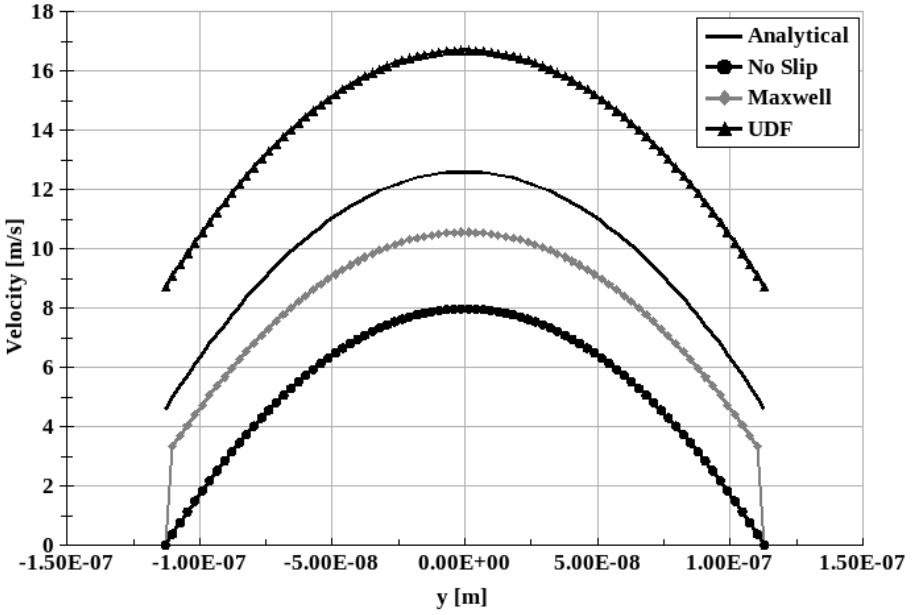

Figure 4: Kn = 0.15 first order analytical, Maxwell, no-slip and UDF velocity profiles on the refined mesh.

At the smaller Knudsen number, Kn = 0.05, the velocity profiles for the first and second order models can be seen in figure 5. The velocity profiles with the acceptation of the second order UDF model are in good agreement, they predict the flow very well together with minor differences at the velocity profile peaks. The second order UDF over-predicts the velocity profile somewhat by approximately 2 ms^{-1}.

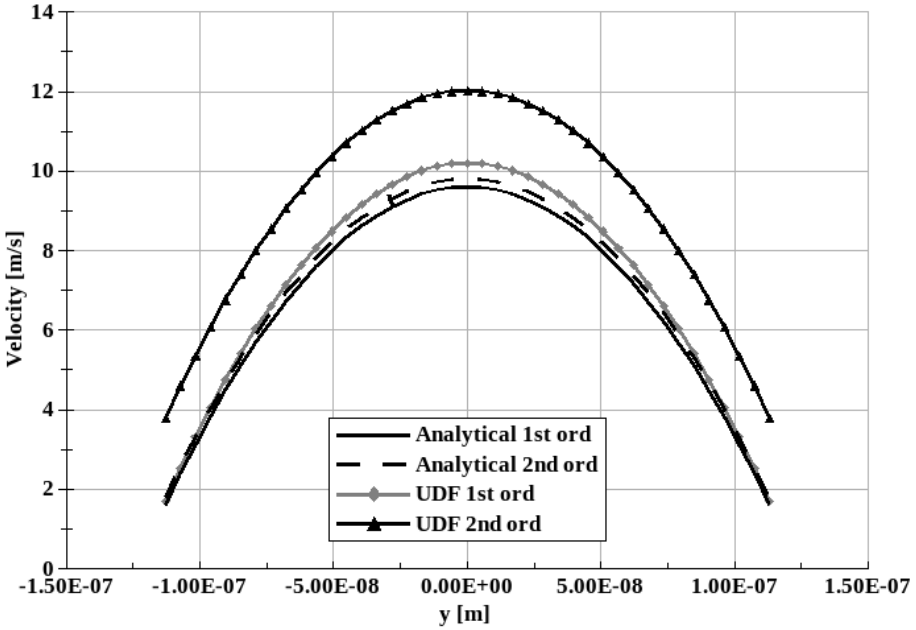

Figure 5: Kn = 0.05 first and second order analytical and UDF velocity profiles.

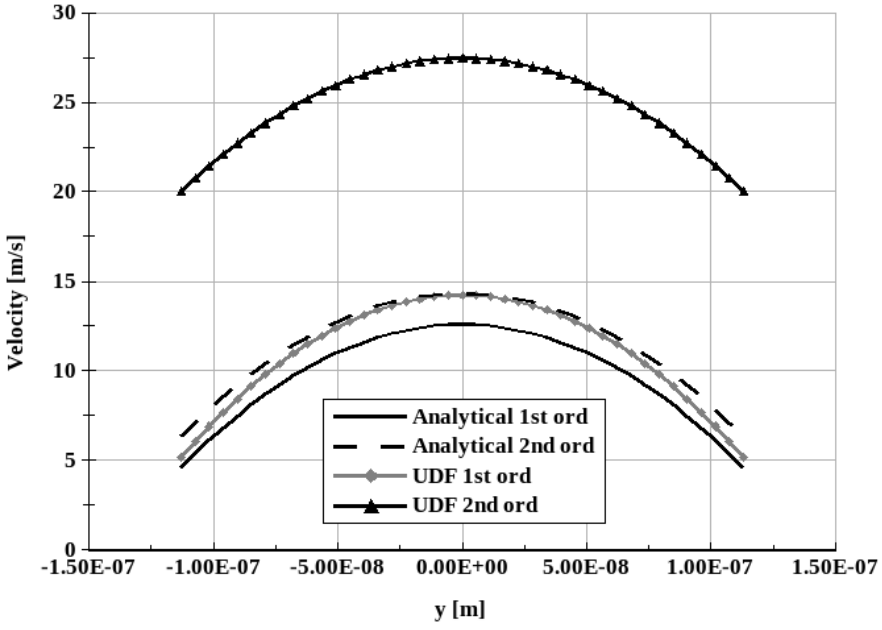

Figure 6: Kn = 0.15 first and second order analytical and UDF velocity profiles.

Investigating second order models for the Knudsen number, Kn = 0.15, seen in figure 6 showed goo agreement with the acceptation of the second order UDF which over-predicted the velocity profile. The second order analytical solution demonstrated a fast velocity profile than the first order, and the first order UDF model fell in the intermediate region between. The choices of constants (A_1 and A_2) become very important regarding the second order models, this is one possible reason for the discrepancy. The flow is in the transition region and therefore creep flow becomes more crucial and difficult to model correctly.

	40×100	80×200	Deviation (%)
No-Slip	3.55×10^{-6}	2.95×10^{-6}	-17.05
Maxwell 1^{st} (FLUENT)	6.05×10^{-6}	4.45×10^{-6}	-26.46
UDF 1^{st}	5.99×10^{-6}	7.77×10^{-6}	29.77
UDF 2^{nd}	1.33×10^{-5}	1.71×10^{-5}	28.14

Table 3: Percentage deviations from the one another for the successive mesh refinement regarding the mass flow rate.

	Kn = 0.05 Mass Flow	Dev. (%)	Kn = 0.15 Mass Flow	Dev. (%)
No-Slip	8.85×10^{-6}		3.55×10^{-6}	
Maxwell 1^{st} (FLUENT)	1.14×10^{-5}	28.24	6.05×10^{-6}	70.17
UDF 1^{st}	1.13×10^{-5}	27.46	5.99×10^{-6}	68.58

Table 4: Percentage deviations from the no-slip value for first order varying Knudsen numbers.

Constants		Kn=0.05		Kn=0.15	
A_1	A_2	UDF	Dev. (%)	UDF	Dev. (%)
1	$5\pi/12$	1.42×10^{-5}	60.5	1.33×10^{-5}	275.63
1	9/8	1.35×10^{-5}	52.71	1.16×10^{-5}	227.02
1	0.5	1.24×10^{-5}	40.09	8.82×10^{-6}	148.15
1	2/9	1.13×10^{-5}	27.46	5.99×10^{-6}	68.58
1	0.0	1.13×10^{-5}	27.46	5.99×10^{-6}	68.58

Table 5: Percentage deviations from the no-slip value for second order varying coefficient constants.

In the above tables, it is clear to see that as the flow moves away from the continuum state of flow, regarding its Knudsen number, the values of the mass flow rate deviate more so from that of the no-slip condition. Table 5 illustrates this with the most emphasis, as the the deviation recorded with the higher Knudsen number produces a larger magnitude than that of the lower. The first order cases seen in table 4 also make similar findings. It is seen in table 3 also that with a coarser mesh, better results are achieved regarding their similarity with the analytical results. This highlights the importance of mesh quality, demonstrating that a finer mesh isn't necessarily a better mesh.

Conclusion & Final Remarks

All simulations and the analytical solutions were found to behave accordingly regarding the expected creep in the wall regions as the flow physics drifted away from the continuum hypothesis assumption. The larger Knudsen number flow demonstrated this effect with more conviction as one would imagine. This is also reinforced via the alterations in the mass flow rate when compared to the no-slip model. The largest Knudsen number reported a maximum of 275.63% deviation from the no-slip model whereas the smaller Knudsen number only reported a maximum of 60.5% deviation.

The finer mesh proved damaging to the flow physics, as it severely reduced the accuracy when compared to the analytical solution.

It was also found regarding the second order models that the choices of constants (A_2) play an important role in the accuracy of the simulations. There is no concrete rule to choose which value to use, highlighting the difficulty of the modelling of this kind of flow problem. It was found however that the constants $A_1 = 1$ and $A_2 = 5\pi/12$ provided the most insightful results.

References

[1] S.S.Mehendale, A.M.Jacobi, R.K.Shah, *Fluid flow and heat transfer at micro- and meso-scales with application to heat exchanger design*, American Society of Engineers, Applied Mechanical Review, Vol. 53, No. 7, 2000.

[2] S.Kandlikar, S.Garimella, D.Li, S.Colin, M.R.King, *Heat Transfer and Fluid Flow in Minichannels and Microchannels*, Elsevier Ltd., First Edition, 2006.

[3] M.C.Potter, *Thermodynamics Demystified*, McGraw-Hill, First Edition, 2009.

[4] J.F.Wendt (Editor), *Computational Fluid Dynamics*, Springer, Third Edition, 2009.

[5] *ANSYS FLUENT Theory Guide*, Release 14.0, November 2011, `http://www.ansys.com`, ANSYS, Inc.

[6] W-M.Zhang, G.Meng, X.Wei, *A review on slip models for gas microflows*, Microfluid Nanofluid (2012) 13:845-882, DOI 10.1007/s10404-012-1012-9, Springer-Verlag, Review Paper.

[7] R.W.Barber, D.R.Emerson (2006), *Challenges in Modelling Gas-Phase Flow in Microchannels: From Slip to Transition*, Heat Transfer Engineering, 27:4, 3-12, DOI: 10.1080/01457630500522271.

[8] J.C.Maxwell, *On Stresses in Rarefied Gases Arising from Inequalities of Temperature*, Phil. Trans. R. Soc. London, vol. 170, pp. 231-256, 1879.

[9] R.Schamberg, *The Fundamental Differential Equations and the Boundary Conditions for High Speed Slip-Flow, and Their Application to Several Specific Problems*, Ph.D thesis, California Institute of Technology, 1947.

[10] C.Cercignani, A.Daneri, *Flow of a Rarefied Gas between Two Parallel Plates*, J. Applied Physics, vol. 34, pp. 3509-3513, 1963.

[11] R.G.Deissler, *An Analysis of Second-Order Slip Flow and Temperature-Jump Boundary Conditions for Rarefied Gases*, Int. J. Heat and Mass Transfer, vol 7, pp. 681-694, 1964.

[12] Y.T.Hsia, G.A.Domoto, *An Experimental Investigation of Molecular Rarefaction Effects in Gas Lubricated Bearings at Ultra-Low Clearances*, Trans. ASME, J.Lubrication Tech., vol 105, pp. 120-130, 1983.

[13] G.E.Karniadakis, A.Beskok, *Microflows: Fundamentals and Simulation*, Springer-Verlag, New York, 2002.

[14] D.A.Lockerby, J.M.Reese, D.R.Emerson, R.W.Barber, *Velocity Boundary Condition at Solid Walls in Rarefied Gas Calculations*, Phys. Rev. E, vol. 70, 017303, 2004.

[15] M.C.Potter, *Fluid Mechanics Demystified*, McGraw-Hill, First Edition, 2009.

Appendix A

C code for the first order UDF given by Kandilar, [2]:

```
/************************************************************************
   Slip velocity profile
************************************************************************/
#include "udf.h"

DEFINE_PROFILE(wall_slip_maxwell, thread, position)
{
  double xf[ND_ND];                /* this will hold the face centroid position */
  double xc[ND_ND];                /* this will hold the cell centroid position */
  double rUF, rUs;
  double rUC,rDUDY;
  double rRho,rT,rR,rMu;
  double rL;
  double rS=1.0, rH=0.000000226/40;
  double Pi=3.14159265358979;

/*face in the thread */
  face_t f;
/*cell in the thread */
  cell_t c0;
/*thread pointer */
  Thread *t0;

/*loop over all faces in the thread*/
  begin_f_loop(f, thread)
    {
/*Get current face centroid */
      F_CENTROID(xf,f,thread);
/*Find cell attached to current face */
      c0 = F_C0(f,thread);
/*Find thread containing this cell*/
      t0 = F_C0_THREAD(f,thread);
/*Get adjacent cell centroid */
      C_CENTROID(xc,c0,t0);
/*Get velocity in the adjacent cell*/
      rUC=C_U(c0,t0);
/*Get velocity y-derivative in the adjacent cell*/
/*      rDUDY=C_DUDY(c0,t0);
/*Get density in the current face cell*/
      rRho=F_R(f,t0);
/*Get temperature in the current face cell*/
      rT=F_T(f,t0);
/*Get gas constant in the current cell*/
      rR=C_RGAS(c0,t0);
```

```
/*Get viscosity in the current cell*/
      rMu=C_MU_L(c0,t0);
/*Get lambda in the current cell*/
      rL=sqrt(Pi/2)*rMu/(rRho*sqrt(rR*rT));
/*compute face velocity*/
  rUF=(2*rUC*rL*(-2+rS))/(-4*rL-rH*rS+2*rL*rS);
/* You can print values to the fluent window, for example */
/*
      printf("Face center: %i Cell Center: %i\n",f,c0);

*/
/* set the current value to be returned for this face */
      F_PROFILE(f, thread, position) = rUF;

  }
  end_f_loop(f, thread)
}
```

Appendix B

C code for the second order UDF given by Kandilar, [2]:

```
/************************************************************************
   Slip velocity profile
************************************************************************/
#include "udf.h"

DEFINE_PROFILE(wall_slip_maxwell_2nd, thread, position)
{
  double xf[ND_ND];               /* this will hold the face centroid position */
  double xc[ND_ND];               /* this will hold the cell centroid position */
  double rUF, rUs;
  double rUC,rDUDY;
  double rRho,rT,rR,rMu;
  double rL;
  double rS=1.0, rH=0.000000226/40;
  double Pi=3.14159265358979;

/*face in the thread */
  face_t f;
/*cell in the thread */
  cell_t c0;
/*thread pointer */
  Thread *t0;

/*loop over all faces in the thread*/
  begin_f_loop(f, thread)
    {
/*Get current face centroid */
      F_CENTROID(xf,f,thread);
/*Find cell attached to current face */
      c0 = F_C0(f,thread);
/*Find thread containing this cell*/
      t0 = F_C0_THREAD(f,thread);
/*Get adjacent cell centroid */
      C_CENTROID(xc,c0,t0);
/*Get velocity in the adjacent cell*/
      rUC=C_U(c0,t0);
  rUF=F_U(f,t0);
/*Get velocity y-derivative in the adjacent cell*/
/*      rDUDY=C_DUDY(c0,t0);
/*Get density in the current face cell*/
      rRho=F_R(f,t0);
/*Get temperature in the current face cell*/
      rT=F_T(f,t0);
/*Get gas constant in the current cell*/
```

```
      rR=C_RGAS(c0,t0);
/*Get viscosity in the current cell*/
      rMu=C_MU_L(c0,t0);
/*Get lambda in the current cell*/
      rL=sqrt(Pi/2)*rMu/(rRho*sqrt(rR*rT));
/*compute face velocity*/
  rUF=(rL*rUC*(-2/9*rL+2*1*rH))/(-2/9*rL*rL+2*1*rH*rL+rH*rH);
/* You can print values to the fluent window, for example */
/*
      printf("Face center: %i Cell Center: %i\n",f,c0);

*/
/* set the current value to be returned for this face */
      F_PROFILE(f, thread, position) = rUF;

  }
  end_f_loop(f, thread)
}
```